Research Article

Preferential Selectivity of Inhibitors with Human Tau Protein Kinase Gsk3β Elucidates Their Potential Roles for Off-Target Alzheimer's Therapy

Jagadeesh Kumar Dasappa and H. G. Nagendra

Department of Biotechnology, Sir M. Visvesvaraya Institute of Technology, Hunasamaranahalli, Via Yelahanka, Bangalore 562157, India

Correspondence should be addressed to Jagadeesh Kumar Dasappa; jk4you@sirmvit.edu

Alzheimer's disease (AD) is a neurodegenerative disorder characterized by the accumulation of amyloid beta peptides (Aβ) and neurofibrillary tangles (NFTs). The abnormal phosphorylation of tau leads to the formation of NFTs produced by the action of tau kinases, resulting in the loss of neurons and synapse, leading to dementia. Hence, tau kinases have become potential drug target candidates for small molecule inhibitors. With an aim to explore the identification of a common inhibitor, this investigation was undertaken towards analyzing all 10 tau kinases which are implicated in phosphorylation of AD. A set of 7 inhibitors with varied scaffolds were collected from the Protein Data Bank (PDB). The analysis, involving multiple sequence alignment, 3D structural alignment, catalytic active site overlap, and docking studies, has enabled elucidation of the pharmacophoric patterns for the class of 7 inhibitors. Our results divulge that tau protein kinases share a specific set of conserved structural elements for the binding of inhibitors and ATP, respectively. The scaffold of 3-aminopyrrolidine (inhibitor 6) exhibits high preferential affinity with GSK3β. Surprisingly, the PDB does not contain the structural details of GSK3β with this specific inhibitor. Thus, our investigations provide vital clues towards design of novel off-target drugs for Alzheimer's.

1. Introduction

Alzheimer's disease is the most common form of neurodegenerative disorders [1] characterized by the formation of extracellular deposits composed of amyloid beta peptide (Aβ) [2] and masses of paired, helically wound protein filaments in the cytoplasm of neuronal cell bodies and neuritic processes called neurofibrillary tangles [3]. These NFTs are formed as a result of hyperphosphorylation of tau protein [4]. The tau proteins are phosphoproteins whose levels of phosphorylation are regulated by tau kinases and phosphatases [5]. Substantial evidence reveals the increased activity of glycogen synthase kinase 3β (GSK3β) (also known as human tau protein kinase I) during AD. Similarly, P25/cyclin-dependent kinase 5 (Cdk5), dual-specific tyrosine [Y] regulated kinase 1A (Dyrk1A), and mitogen-activated protein kinases (MAPK) also possess higher activity in AD brain [6].

Thus, our work focuses on the chosen 10 kinases involved in hyperphosphorylation of tau and elevated responses in AD [7]. Kinase holds a large gene family and these domains are alike in sequence and structure. Developments of discriminating inhibitors are a key task in drug discovery and development, and appreciating the basis of kinase inhibitor selectivity is critical to the design of effective drugs.

GSK3β is composed of three domains: an N-terminal domain consisting of a closed β-barrel structure, a C-terminal domain containing a "kinase fold" structure, and a small extradomain subsequent to the C-terminal domain. The catalytic site is between the two major domains and has an ATP analogue molecule in its ATPbinding site. The adenine ring is buried in the hydrophobic pocket and interacts specifically with the main-chain atoms of the hinge loop [8]. The structure of GSK3β is known to have a catalytically active dimer conformation that progressively phosphorylates

TABLE 1: Details of 10 tau kinases used in the analysis.

Sl. number	Protein name	UniProt ID	PDB ID	Number of residues	Ligand present in the PDB structure	Nomenclature of inhibitors in the study
(1)	Glycogen synthase kinase 3 beta (GSK3β)	P49841	1J1C	420	Adenosine-5′-diphosphate	—
(2)	Cyclin-dependent kinase 5 (CDK5)	Q00535	3O0G	292	4-Amino-2-[[4-chlorophenyl]amino]-1,3-thiazol-5-yl][3-nitrophenyl]methanone	Inhibitor 1
(3)	p38 delta kinase (p38)	O15264	3COI	365	No Ligand	—
(4)	Mitogen-activated protein kinase 1 (Erk1/2)	P28482	1TVO	360	5-[2-Phenylpyrazolo[1,5-a]pyridin-3-yl]-1h-pyrazolo[3,4-c]pyridazin-3-amine [Drug Bank ID DB07794]	Inhibitor 2
(5)	Mitogen-activated protein kinase 10 (JNK3)	P53779	2O0U	464	N-{3-Cyano-6-[3-[1-piperidinyl]propanoyl]-4,5,6,7-tetrahydrothieno[2,3-c]pyridin-2-yl}1-naphthalenecarboxamide	Inhibitor 3
(6)	Casein kinase 1 delta (CK1d)	P48730	3UYT	415	4-[1-Cyclohexyl-4-[4-fluorophenyl]-1H-imidazol-5-yl]pyrimidin-2-amine	Inhibitor 4
(7)	Dual-specificity tyrosine-[Y]-phosphorylation-regulated kinase 1A (DYRK1A)	Q13627	3ANR	763	7-Methoxy-1-methyl-9h-beta-carboline [harmine complex] [Drug Bank ID DB07919]	Inhibitor 5
(8)	Protein kinase A (PKA)	P17612	3MVJ	351	[3R]-1-[5-Methyl-7H-pyrrolo[2,3-d]pyrimidin-4-yl]pyrrolidin-3-amine	Inhibitor-6 (3-aminopyrrolidine scaffold)
(9)	Protein kinase B (PKB/AKT)	P31749	3MV5	480	[3R]-1-[5-Methyl-7H-pyrrolo[2,3-d]pyrimidin-4-yl]pyrrolidin-3-amine	Inhibitor-6 (3-aminopyrrolidine scaffold)
(10)	Protein kinase C alpha (PKC)	P17252	3IW4	672	3-[1H-Indol-3-yl]-4-[2-[4-methylpiperazin-1-yl]quinazolin-4-yl]-1H-pyrrole-2,5-dione	Inhibitor 7

substrates with Ser/Thr penta repeats [9]. It is known that the inhibitors compete with the ATP binding sites of GSK3β [10, 11]. Realizing the need to design the inhibitors for these kinases, with the hope that it could affect the hyperphosphorylation of tau, the investigations have been undertaken. The studies reveal shared conservations across sequences, structural homologies, and ATP binding site geometries across the ten tau kinases. Interestingly, the inhibitor 3-aminopyrrolidine scaffold exhibits high preferential affinity with GSK3β. Though the literature on AD indicates overexpression and activity of GSK3β during pathogenesis of AD, surprisingly, the PDB does not contain the structural details of GSK3β with these specific inhibitors. Consequently, our explorations provide vital clues towards design of novel off-target drugs for AD.

2. Materials and Methods

The analysis of the structures of the 10 tau kinases, along with their respective ligands, was carried out as illustrated in the flow chart (Figure 1). To begin with, the structures of the 10 tau kinases, along with their respective ligands, were retrieved

from the PDB and their details are provided in Table 1. A Phylogenetic tree was generated for the amino acid sequences of 10 tau kinases using CLUSTALW [12] and is illustrated in Figure 2. The dendrogram reveals that GSK3β, CDK5, MAPK such as p38, extracellular signal-regulated kinases 1 & 2 (ERK 1/2), c-Jun N-terminal kinase (JNK), and dual-specificity tyrosine-[Y]-phosphorylation-regulated kinase 1A (DYRK1A) are closely related (as in cluster 1); protein kinase A (PKA), protein kinase B (AKT/PKB), and protein kinase C (PKC) form the closely related second cluster. Interestingly, casein kinase 1 delta (CK1d) stands out as an independent taxis, indicating characteristic sequence variations from the group.

To observe the conservation of residues in the ATP binding region, a multiple sequence alignment was carried out amongst the 10 kinases, using the tool MultAlin [13]. The alignment is depicted in Figure 3(a), which reveals that the sequences differ significantly at the positions of gatekeeper residues and the surface residues, while they are well conserved at the subsites that interact directly with ATP. The ATP binding amino acids LYS 85 & ASP 200, ASP 133 & VAL 135 and GLU 185 are conserved across these kinases, and lie in

TABLE 2: Percentage identity, similarity, and RMSD values (for the overlapping number of atoms).

	GSK3β	CDK5	P38	ERK1/2	JNK	CK1d	DYRK1A	AKT	PKA
CDK5	[#]35.6% [@]66.0% [*]1.25 (238)	—	—	—	—	—	—	—	—
P38	32.3% 62.0% [*]1.45 (221)	36.4% 64.9% [*]1.52 (202)	—	—	—	—	—	—	—
ERK1/2	32.8% 64.5% [*]1.43 (252)	37.6% 68.0% [*]1.42 (233)	49.0% 77.4% [*]1.60 (277)	—	—	—	—	—	—
JNK	28.0% 54.8% [*]1.59 (238)	35.4% 64.3% [*]1.61 (228)	47.7% 75.3% [*]1.65 (265)	43.1% 73.8% [*]1.46 (287)	—	—	—	—	—
CK1d	25.3% 49.6% [*]1.64 (205)	22.8% 48.1% [*]1.60 (200)	25.6% 54.0% [*]1.72 (167)	29.5% 50.4% [*]1.75 (195)	24.6% 50.8% [*]1.76 (188)	—	—	—	—
DYRK1A	28.4% 53.2% [*]1.29 (253)	30.4% 7.5% [*]1.34 (243)	29.1% 53.6% [*]1.52 (218)	28.3% 57.1% [*]1.39 (246)	28.9% 52.3% [*]1.72 (247)	24.5% 51.8% [*]1.57 (213)	—	—	—
AKT	27.0% 48.4% [*]1.55 (222)	25.4% 57.4% [*]1.47 (214)	26.1% 56.7% [*]1.61 (205)	22.8% 53.1% [*]1.48 (231)	26.3% 52.5% [*]1.64 (221)	25.8% 54.5% [*]1.68 (207)	26.0% 56.4% [*]1.36 (230)	—	—
PKA	26.4% 59.2% [*]1.56 (213)	23.4% 58.9% [*]1.50 (207)	26.6% 59.4% [*]1.65 (183)	24.1% 53.9% [*]1.65 (214)	26.3% 52.9% [*]1.72 (194)	26.1% 53.8% [*]1.76 (207)	26.0% 57.1% [*]1.50 (219)	45.6% 77.2% [*]1.21 (292)	—
PKC	24.8% 51.8% [*]1.52 (223)	27.8% 61.9% [*]1.45 (214)	27.9% 56.4% [*]1.65 (203)	23.9% 56.2% [*]1.68 (228)	24.6% 50.8% [*]1.82 (221)	23.5% 55.8% [*]1.70 (208)	25.9% 56.7% [*]1.43 (224)	47.4% 79.2% [*]1.07 (285)	32.8% 60.3% [*]1.37 (279)

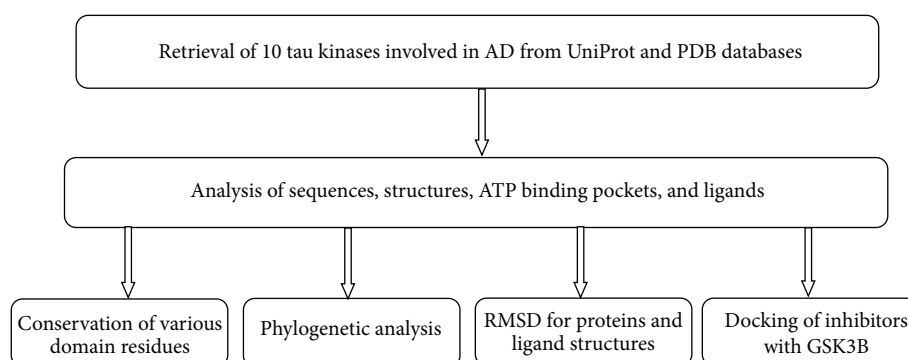[#]Identity, [@]similarity, and [*]RMSD (total number of atoms involved).
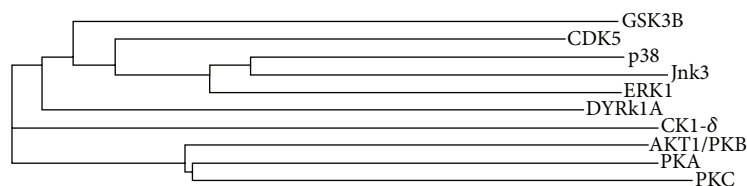

FIGURE 1: Work flow chart.

FIGURE 2: Phylogenetic tree generated for sequences of the tau kinases using CLUSTALW software.

TABLE 3: Structures of 7 potential small molecule inhibitors and their relative binding affinities (IC_{50} and K_i) values.
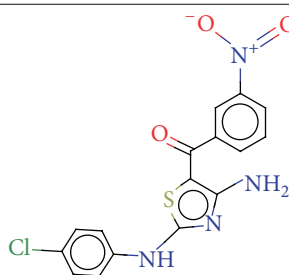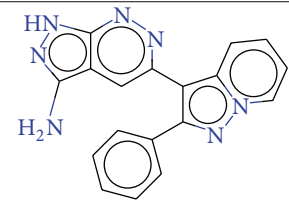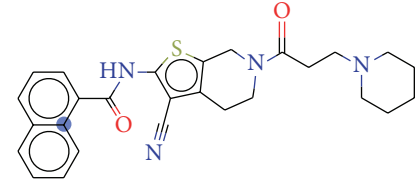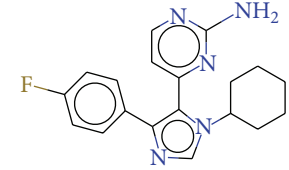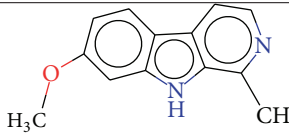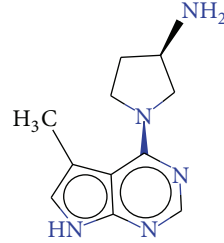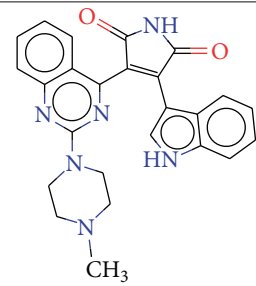
Sl. number	Ligand	Molecular formula	Molecular weight (Da)	IC_{50}-median inhibition concentration value	K_i-inhibition constant value
(1)		[$C_{16} H_{11} Cl N_4 O_3 S$] [Drug Bank ID DB07794]	374.80	2000 nM	600 nM
(2)		[$C_{18} H_{13} N_7$]	327.34	1900 nM	140 nM
(3)		[$C_{27} H_{28} N_4 O_2 S$]	472.60	3200 nM	3200 nM
(4)		[$C_{19} H_{20} F N_5$]	337.39	130 nM	n/a
(5)		[$C_{13} H_{12} N_2 O$] [Drug Bank ID DB07919]	212.25	350 nM	n/a
(6)		[$C_{11} H_{15} N_5$]	217.27	3200 nM	n/a
(7)		[$C_{25} H_{22} N_6 O_2$]	438.48	2.1 nM	n/a

TABLE 4: RMSD values of ATP and the seven kinase inhibitors amongst each other.

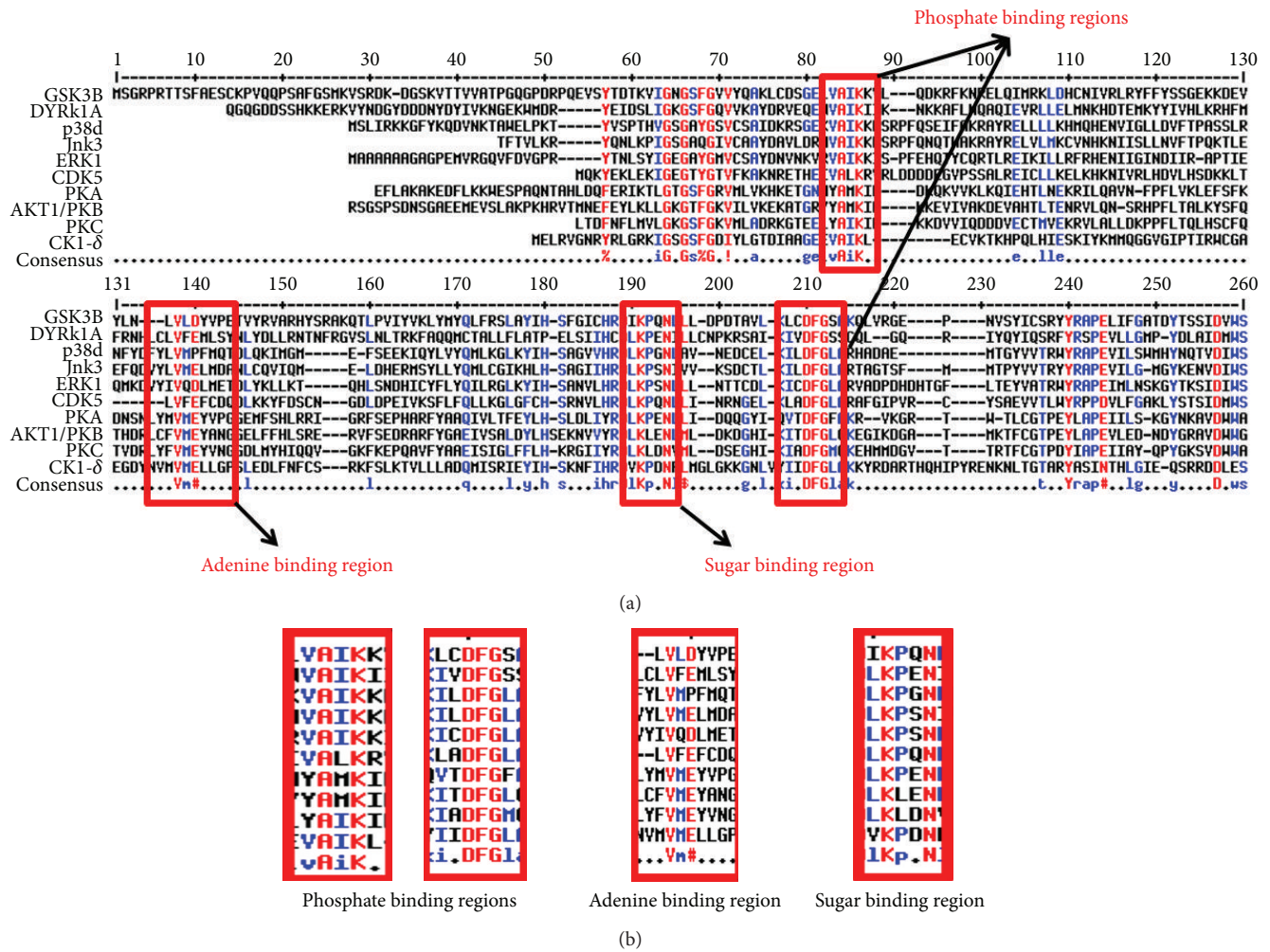|	Inhibitor 1	Inhibitor 2	Inhibitor 3	Inhibitor 4	Inhibitor 5	Inhibitor 6	Inhibitor 7
Inhibitor 1	—	—	—	—	—	—	—
Inhibitor 2	0.57	—	—	—	—	—	—
Inhibitor 3	0.46	0.32	—	—	—	—	—
Inhibitor 4	0.56	0.66	0.54	—	—	—	—
Inhibitor 5	0.43	0.41	0.33	0.52	—	—	—
Inhibitor 6	0.51	0.39	0.46	0.49	0.49	—	—
Inhibitor 7	0.53	0.54	0.41	0.54	0.41	0.55	—
ATP	0.37	0.64	0.58	0.54	0.51	0.67	0.48

FIGURE 3: (a) Alignment of tau kinases showing the conserved residues in the ATP binding region. (b) Highlight of sequence conservation across ATP binding residues.

the phosphate binding region, adenine binding region and in the sugar binding regions respectively (refer to Figure 3(b)). Overall sequence identity and similarity amongst the sequences and RMSD between the 3D geometries are highlighted in Table 2. The identity (and similarity) amongst the kinase sequences lies in the broad range of 22.8% (48.1%) and 49% (77.4%). The closest set appears between ERK1/2 and P38, which share the highest identity of 49%, while the least

values of 22.8% exist between 2 sets, namely, CK1d and CDK5 and AKT and ERK1/2, respectively. The structural alignment to calculate the RMSD values was carried out using MultiProt [14]. It is interesting to note that the RMSD between all pairs of 10 tau kinases for $C\alpha$ atoms range between 1.07 and 1.82 Å (refer to Table 2). Interestingly, these lowest and highest values of RMSD are related to the molecule PKC. However as expected, for the molecule CK1d which stands

Table 5: Interaction of binding site residues amongst the 10 tau kinases with ATP.

GSK3β	CDK5	P38	ERK1/2	JNK	CK1d	DYRK1A	AKT	PKA	PKC	ATP binding site conservation across the 10 kinases
#I 62 * [4.4]	I10 [5.70]	V31 [4.24]	I31 [5.59]	I70 [4.23]	I15- [2.36]	I165- [3.09]	L156 [4.34]	L49 [4.10]	L345 [4.70]	I/V/L
#G 63 * [5.4]	G11 [4.7]	G32 [3.97]	G32 [>6]	G71 [4.31]	G16 [3.24]	G166 [5.12]	G157 [3.95]	G50 [4.88]	G346 [4.81]	G-well conserved
#N 64 * [5.24]	—	S33 [3.93]	E33 [>6]	—	—	K167 [4.60]	K158- [2.95]	T51 [2.76]	K347 [5.88]	Not conserved
#G 65 * [4.03]	—	G34 [3.36]	Y36 [2.79]	—	—	G168 [5.72]	G159 [5.08]	G52 [3.90]	G348 [>6]	Not conserved
#S 66 * [2.82]	—	A35 [3.64]	—	—	—	SI69 [>6]	—	S53 [4.59]	S349 [5.81]	Not conserved
#F 67 * [3.21]	—	Y36 [3.17]	—	—	F20 [5.54]	F170 [>6]	F161 [5.54]	F54 [3.82]	—	Not conserved
#V 70 * [5.9]	V18- [2.72]	V39 [2.89]	V39 [2.79]	V78 [>6]	I 23 [5.07]	V173 [>6]	V164 [4.93]	V57 [2.88]	V353 [4.80]	V/I
#A 83 * [5.46]	A31 [4.61]	A52 [4.93]	A52 [4.64]	A91 [5.99]	A 36 [5.42]	A186 [5.00]	A177 [4.90]	A70 [4.49]	A366 [4.51]	A-well conserved
#K 85 * [2.64]	K33 [4.28]	K54- [2.67]	K54- [2.93]	K93 [5.18]	K38 [3.23]	K188 [3.19]	I179 [5.23]	K72- [3.72]	K368- [2.31]	K-well conserved
#E 97 * [4.59]	E51 [>6]	E72 [4.96]	E71 [3.71]	E111 [5.66]	E52 [3.78]	E203 [3.24]	E198 [4.93]	E91 [5.32]	E387 [3.45]	E-well conserved
#V 110 * [5.1]	V64 [>6]	I85 [>6]	I84 [>6]	I124 [>6]	P66 [>6]	V222 [5.80]	T211 [4.13]	V104 [5.40]	T401 [3.29]	V/I/P/T
#L 132 * [5.7]	F80 [4.31]	M107 [5.06]	Q105- [2.29]	M146- [2.18]	M82- [2.40]	F238 [4.71]	M227 [4.36]	M120 [4.50]	M417 [3.24]	F/Q/M
#D 133 * [2.58]	E81- [2.86]	P108- [2.49]	D106- [2.96]	E147 [5.39]	E-83- [2.83]	E239- [2.54]	E228- [2.88]	E121- [2.52]	E418- [3.05]	D/E-well conserved
#Y 134 * [3.9]	F82 [5.08]	F109 [4.65]	L107 [3.03]	L148 [3.63]	L84 [4.73]	M240 [3.57]	Y229 [3.81]	Y122 [5.50]	Y419 [3.44]	F/L/M/Y
#V 135 * [3.05]	C83- [3.19]	M110- [3.13]	M108- [3.03]	M149- [2.51]	L85- [2.97]	L241- [2.84]	A230- [3.20]	V123- [2.69]	V420- [2.64]	C/M/L/A/V
#T 138 * [5.6]	D86- [2.74]	D113- [2.89]	D111- [2.77]	N152- [2.45]	S88- [2.91]	N244 [4.37]	E 234- [2.63]	E127- [3.01]	D424- [2.99]	D/N/S/E
#R 141 * [3.10]	K89 [5.45]	K116 [5.32]	K 114 [3.92]	Q155 [4.03]	D 91 [4.42]	D247 [5.51]	F237 [4.76]	S130 [5.50]	Y427 [>6]	R/K/Q/D/F/S/Y
#Q 185 * [2.98]	Q130- [2.66]	G 154 [4.71]	SI53- [2.71]	S193 [4.42]	D132 [3.84]	E291 [4.66]	E278- [3.11]	E170 [2.30]	D467- [3.23]	Q/G/S/D/E
#N 186 * [3.45]	N131 [4.33]	N155 [>6]	N154 [3.98]	N194 [4.09]	N133 [2.88]	N292 [3.39]	N279 [5.38]	N171 [3.22]	N468 [4.22]	N-well conserved
#L 188 * [5.8]	L133 [5.76]	A157 [5.79]	L156 [>6]	V196 [>6]	L135 [5.29]	L 294 [>6]	M281 [5.54]	L173 [5.88]	M470 [4.33]	L/A/V/M
#C 199 * [4.63]	A143 [5.93]	L167 [>6]	C166 [4.09]	L206 [5.20]	I148 [6.06]	V306 [2.70]	T291 [3.83]	TI83 [3.62]	A480 [4.27]	C/A/L/I/V/T
#D 200 * [4.84]	N144 [3.72]	D168 [5.04]	D167 [3.79]	D207 [4.19]	D149 [2.97]	D307- [2.72]	D292 [3.11]	D184 [3.96]	D481- [2.59]	D-well conserved
22	16	19	16	15	18	18	21	22	18	Number of interacting residues with ATP within 6 Å

#Indicates residue type and number; * indicates distances in Angstroms.

TABLE 6: Binding site residues of GSK3β interacting with 7 inhibitors when docked in the ATP Pocket.

Residues in the ATP binding site of GSK3β	ATP	Inhibitor 1	Inhibitor 2	Inhibitor 3	Inhibitor 4	Inhibitor 5	Inhibitor 6	Inhibitor 7	Number of interactions each residue has across inhibitors (within 6 Å)
I 62	4.4	—	3.62	2.35	4.09	3.98	2.90	2.84	6
G 63	5.4	—	—	—	—	—	4.50	3.20	3
N 64	5.24	—	—	—	—	—	—	4.56	4
G 65	4.03	—	—	—	—	—	—	—	1
S 66	2.82	—	—	—	—	—	—	—	1
F 67	3.21	—	—	—	—	—	—	—	1
V 70	5.9	4.09	—	5.20	—	—	5.37	—	4
A 83	5.46	4.96	5.51	—	5.80	—	5.03	—	5
K 85	2.64	3.03	—	3.21	5.02	—	—	2.84	5
E 97	4.59	—	—	—	—	—	—	—	1
V 110	5.1	—	3.35	—	—	—	—	—	2
L 132	5.7	—	4.41	5.69	—	—	5.11	—	4
D 133	2.58	2.62	2.88	3.21	2.87	—	3.03	—	6
Y 134	3.9	—	—	—	2.77	—	5.65	—	3
V 135	3.05	2.39	2.90	2.65	2.72	4.81	2.59	5.72	8
T 138	5.6	—	—	—	—	—	—	—	1
R 141	3.12	4.91	2.17	—	3.75	4.51	5.15	3.81	7
Q 185	2.98	—	—	2.99	5.89	—	2.94	2.90	5
N 186	3.45	—	—	4.64	—	—	4.368	—	3
L 188	5.8	4.03	5.12	—	—	—	—	—	3
C 199	4.63	4.05	—	—	—	—	—	—	2
D 200	4.84	2.70	4.57	3.45	—	—	—	—	4
Number of interacting residues across various inhibitors (within 6 Å)	22	9	9	9	8	3	11	7	—

out in the phylogeny, the identities with all other kinases are less than 30%. Similarly, the RMSD values of all the kinases with CK1d lie in the higher range of 1.57 to 1.76 Å. Further, the structural alignments revealed that the active site occurs between two lobes of kinases showing the conserved overlap of the ATP binding regions. Thus, the RMSD values for the entire ATP binding region amongst the kinases lie between 0.63 and 1.25 Å. However, the RMSD values for the phosphate binding region lie between 0.23 and 0.46 Å, and the nucleotide binding region is in-between 0.16 and 1.25 Å respectively. Hence, docking the binding site of kinases with ATP was attempted to appreciate the nature of interactions. Table 3 provides the molecular details and properties of the various inhibitors used in the study. Their relative binding affinities in terms of IC50 and K_i values are also indicated for each inhibitor (Table 3). The set of chosen inhibitors does contain two small molecules which are deposited in the drug bank, that is, inhibitor 2 (Drug Bank ID DB07794) and inhibitor 5 (Drug Bank ID DB07919). In order to appreciate

the structural similarity of these inhibitors with ATP, 3D alignments were carried out across the 7 kinase inhibitors and ATP. The outcome of these structural comparisons revealed that the RMSD between ATP and the 7 ligands lie between 0.37 and 0.67 Å, while the inhibitor-to-inhibitor RMSD values are in the range of 0.32 to 0.67 Å. All the RMSD values are consolidated in Table 4.

The ATP binding site of GSK3β spans a long stretch containing 22 residues. Table 5 lists the various residues forming the ATP binding pocket and exhibiting favorable interactions with ATP. In order to appreciate the conservation of this ATP binding site across all 10 tau kinases, ATP molecule was docked and all plausible interactions within 6 Å were tabulated. Docking studies were carried out using the Discovery Studio software Version 3.5 (Accelrys Software Inc., USA) and Lead IT tool of FlexX 2.1.2. It is clear from Table 5 that G63, A83, K85, E97, D/E133, N186, and D200 form the set of well-conserved residues in the ATP binding pocket and interact with ATP in all the 10 kinases. Though

the molecules JNK and ERK1/2 exhibit less number of interactions with ATP, key contacts of conserved residues are indeed present. Residue corresponding to V110 exhibits least number of interactions across kinases. Though the residue corresponding to R141 appears changed in all the kinases, its interactions with ATP, across the receptors, are well conserved.

Our aim to study the efficacies of select inhibitors with GSK3β triggered the need to dock these ligands to the key tau kinase GSK3β. Identifying the ATP binding site, the molecular docking studies of kinase inhibitors were carried out using the Discovery Studio software Version 3.5 and Lead IT tool of FlexX 2.1.2. GSK3β receptor structure was docked to all of the seven ligands to the ATP binding pocket by the rigid receptor-flexible ligand docking competencies of FlexX and the interactions are tabulated in Table 6. The docking examination revealed that the inhibitor-3-aminopyrrolidine scaffold exhibits high preferential affinity with GSK3β. While all inhibitors appear to sit in the ATP pocket of GSK3β, the most favorable is inhibitor 6 and the least probable is inhibitor 5.

3. Results and Discussion

In the present study, the analysis of 10 tau kinases implicated in AD has been performed to elucidate the conservation of the binding site and selectivity of the 7 inhibitors. Multiple sequence alignment, 3D structural alignment, catalytic active site overlap, and docking studies of inhibitors with GSK3β have been carried out to fingerprint the interactions with the key/gatekeeper residues in the ATPbinding pocket. The results highlight that tau protein kinases share common structural elements for the binding of the inhibitors and ATP. Comparatively, the inhibitor 3-aminopyrrolidine (inhibitor 6) exhibits high preferential affinity with GSK3β. Interestingly, the literature on AD indicates the overexpression and activity of GSK3β during pathogenesis of AD, and surprisingly, the PDB does not contain the structural details of GSK3β with this specific inhibitor. Our studies disclose that regions of the active site which found high conservation across tau kinases may form the determinants for binding to the ligand. Interactions of 7 inhibitors with the remaining 9 tau kinases in AD are also being explored.

4. Conclusions

Our results indicate that the binding pocket of the 10 tau kinases is structurally conserved and offer a common feature of determinants with the 7 inhibitors investigated. Specific analysis with GSK3β reveals preferential binding to 3-aminopyrrolidine scaffold. This study highlights that suitable therapeutics can be successfully developed from the available chemical space, thus facilitating inhibitor design and off-target effects for AD.

Conflict of Interests

The authors declare that this paper has no conflict of interests with FlexX 2.1.2. and Accelrys Software Inc., USA, version 3.5 software, which is a licensed version.

References

[1] M. L. Hemming, J. E. Elias, S. P. Gygi, and D. J. Selkoe, "Identification of beta-secretase (BACE1) substrates using quantitative proteomics," *PloS ONE*, vol. 4, no. 12, Article ID e8477, 2009.

[2] D. J. Selkoe, "Amyloid β-protein and the genetics of Alzheimer's disease," *The Journal of Biological Chemistry*, vol. 271, no. 31, pp. 18295–18298, 1996.

[3] D. J. Selkoe, "Cell biology of protein misfolding: the examples of Alzheimer's and Parkinson's diseases," *Nature Cell Biology*, vol. 6, no. 11, pp. 1054–1061, 2004.

[4] K. Iqbal, F. Liu, C.-X. Gong, and I. Grundke-Iqbal, "Tau in Alzheimer disease and related tauopathies," *Current Alzheimer Research*, vol. 7, no. 8, pp. 656–664, 2010.

[5] L. Martina, X. Latypovac, C. M. Wilsona et al., "Tau protein kinases: involvement in Alzheimer's disease," *Ageing Research Reviews*, vol. 12, no. 1, pp. 289–309, 2013.

[6] S.-H. Chung, "Aberrant phosphorylation in the pathogenesis of Alzheimer's disease," *BMB Reports*, vol. 42, no. 8, pp. 467–474, 2009.

[7] I. Ferrer, T. Gomez-Isla, B. Puig et al., "Current advances on different kinases involved in tau phosphorylation, and implications in Alzheimer's disease and tauopathies," *Current Alzheimer Research*, vol. 2, no. 1, pp. 3–18, 2005.

[8] M. Aoki, T. Yokota, I. Sugiura et al., "Structural insight into nucleotide recognition in tau-protein kinase I/glycogen synthase kinase 3β," *Acta Crystallographica D*, vol. 60, no. 3, pp. 439–446, 2004.

[9] W. Ji and I. Ha, "Drug development for Alzheimer's disease: recent progress," *Experimental Neurology*, vol. 19, no. 3, pp. 120–131, 2010.

[10] F. Liu, Z. Liang, J. Shi et al., "PKA modulates GSK-3β- and cdk5-catalyzed phosphorylation of tau in site- and kinase-specific manners," *FEBS Letters*, vol. 580, no. 26, pp. 6269–6274, 2006.

[11] A. Martinez, C. Gil, and D. I. Perez, "Glycogen synthase kinase 3 inhibitors in the next horizon for Alzheimer's disease treatment," *International Journal of Alzheimer's Disease*, vol. 2011, Article ID 280502, 7 pages, 2011.

[12] http://www.ebi.ac.uk/Tools/phylogeny/clustalw2_phylogeny/.

[13] F. Corpet, "Multiple sequence alignment with hierarchical clustering," *Nucleic Acids Research*, vol. 16, no. 22, pp. 10881–10890, 1988.

[14] M. Shatsky, R. Nussinov, and H. J. Wolfson, "A method for simultaneous alignment of multiple protein structures," *Proteins*, vol. 56, no. 1, pp. 143–156, 2004.